Techno-Economic Trade-Off between Battery Storage and Ice Thermal Energy Storage for Application in Renewable Mine Cooling System

Sajjan Pokhrel[ID]**, Ali Fahrettin Kuyuk, Hosein Kalantari**[ID] **and Seyed Ali Ghoreishi-Madiseh ***

NBK Institute of Mining Engineering, The University of British Columbia, Vancouver, BC V6T 1Z4, Canada;
sajjan12@mail.ubc.ca (S.P.); alikuyuk@mail.ubc.ca (A.F.K.); hoseink@mail.ubc.ca (H.K.)
* Correspondence: ali.madiseh@ubc.ca

Abstract: This paper performs a techno-economic assessment in deploying solar photovoltaics to provide energy to a refrigeration machine for a remote underground mine. As shallow deposits are rapidly depleting, underground mines are growing deeper to reach resources situated at greater depths. This creates an immense challenge in air-conditioning as the heat emissions to mine ambient increases substantially as mines reach to deeper levels. A system-level design analysis is performed to couple PV with a refrigeration plant capable of generating 200 tonne of ice per day to help to mitigate this issue. Generated ice can directly be used in cooling deep underground mines via different types of direct heat exchangers. State-of-the-art technology is used in developing the model which aims to decrease the size and cost of a conventional refrigeration system run on a diesel generator. Costs associated with deploying a solar system are computed as per the recent market value. Energy savings, carbon emissions reduction, and net annual savings in employing the system are quantified and compared to a diesel-only scenario. In addition, two different energy storage strategies: an ice storage system and a battery storage system, are compared. A detailed economic analysis is performed over the life of the project to obtain the net cash flow diagram, payback period, and cumulative savings for both systems. Moreover, a sensitivity analysis is proposed to highlight the effect of solar intensity on solar system size and the area required for installment. The study suggests that the use of solar PV in mine refrigeration applications is technically feasible and economically viable depending on the sun-peak hours of the mine location. Additionally, the economics of deploying an ice storage system compared to the battery storage system has a better payback period and more cumulative savings.

Keywords: deep mine cooling; solar electric refrigeration; ice thermal energy storage; techno-economic assessment; solar PV design; renewable energy in mining; solar-powered ice maker

1. Introduction

Industrial energy usage accounts for 40% of the overall global energy demand in 2018, greater than any other end-use sectors [1]. Mining is the second most energy-intensive industry after construction, draining 6.2% of the global energy share [2]. Mine ventilation and refrigeration could account for about 30–40% of a deep underground mine's total energy expense [3]. Mines are going deeper and deeper to meet global consumer needs. In ultra-deep mines (2500 m or deeper), gravitational compression of the intake air sinking in the downcast shaft and geothermal heat acting on the mine ambient can cause a substantial increase in the temperature in association with the depth (auto-compression). Additionally, virgin rock temperature in such mines could be as high as 65 °C [4] due to the geothermal gradient. However, regardless of auto-compression impact and virgin rock temperature, mine ambient air wet-bulb temperature should not exceed 28 °C [5]. Consequently, more cooling would be required for

such mines to maintain safe climatic conditions. The design of a mine cooling system is usually based on the peak summer condition to ensure year-round, stable coolth generation. However, a refrigeration scheme designed over peak surface load requires a relatively large size of chillers, cooling towers, and condensers due to overestimation of annual demand. This overestimation is inevitable as the peak load acting on these systems are usually seasonal or happen for a very limited period of the year. This results in redundant project cost and could affect the project feasibility negatively. Fortunately, this problem could be solved by employing a 'by-pass' system that could trim the peak cooling demand and help downsize the capital cost.

The literature suggests that energy savings in a mine ventilation and refrigeration system could be expanded to 22% of the current trend, reducing it from 17.5 MJ/tonne of ore to 13.6 MJ/tonne of ore [6]. Zietsman et al. [7] reports annual savings of ZAR 1.65 million (South African Rand) by implementing peak clipping via thermal storage arrangement in deep platinum mine. Plessis et al. [8] simulated an energy efficiency strategy to forecast the potential savings of implementing a peak shaving strategy in a real-life mine cooling system and concluded that a decrease of 33% is possible in overall electrical energy consumption. A cooling load management initiative taken in two different South African mines has shown that about 25% of electricity savings is an attainable figure in mine refrigeration [9]. Another energy-saving strategy for a mine cooling system with a power usage of 22 MW resulted in 132 GWh savings, equivalent to 30 million ZAR or 38% of annual refrigeration cost [10]. Undoubtedly, gradual deepening of mines calls for more research in energy generation, storage, and management to overcome future mine refrigeration challenges. This paper proposes a strategy to manage the peak cooling demand of a remote underground mine using ice cubes generated from a solar photovoltaics (PV)-driven refrigeration system.

The concept of cooling underground mines via ice goes back to the 1980s [11]. However, back then, the complex and delicate architecture of ice plants made it viable only for mines greater than 3000 m in depth. With improved technology, the reduced cost of mine cooling creates more opportunity to deploy such systems at shallower depths more feasibly. Studies show that the feasible depth has moved from 3000 m in 1980 to 2500 m in 2010 to 1760 m in 2014 [12,13]. It is important to note that such mines otherwise are cooled with chilled air or chilled water from the surface. It is also worthwhile to mention that the specific heat capacity of water and the latent heat of fusion of ice is about 4.2 and 334 times the specific heat capacity of air, respectively. Chilled air is the most cost-effective cooling solution, but lower specific heat capacity makes it unsuitable to remove extra heat from greater depths. Hence, chilled water is used to remove heat at higher depths. However, as the depth further increases, the pumping requirements for returning water from underground leads to considerable operation cost. Due to the higher specific heat capacity of ice over water, the volume of ice required to dissipate an equal amount of thermal energy is between 20% to 30% of the chilled water [14,15]. In such ultra-deep mines, ice is used as a coolant to enhance the system performance. Belle et al. [14] mentions that with the development in technology, the coal mines in the Bowen basin in Australia might have to move towards ice-cooling in the near future. Although notable mines including Phakisa gold mine and Impala gold mine in South Africa are currently using this technology, the potential use of solar electricity for ice generation is a novel concept in mine sites.

1.1. Motivation of the Research

Today, amidst the gradual depletion of mining resources, more and more mine enterprises are moving to remote locations with no electric grid access. In remote sites, fossil fuels including diesel and natural gas are the main sources of energy. In 2017, 18,364 k tonne of diesel is consumed in mining: about 18% of the total industrial share [2]. Diesel emissions are the major contributors to the CO_2 accumulation in the earth's atmosphere by adding 123 ppm between the pre-industrial era and 2016 [16]. In mining, 71% of the emission is from fossil fuels while 29% is due to electricity usage [17]. In addition to its environmental impacts, diesel dependence also created an escalation in the cost of electricity generation from diesel generators. Utility cost of electricity generation from a diesel generator can

be as high as 0.76 USD/kWh for some remote locations excluding carbon tax [18]. Thermal duties of refrigeration units in deep mines are typically in the range of 0.5 and 20 MW [14,19]. The use of diesel generators to generate this huge energy is a financial and an environmental concern. The motivation of the research is the need to lower the high cost of energy that remote mines are currently using in addition to their higher environmental footprints. The penetration of renewable energy in mine chilling application not only assists to break the complicated relationship of mining and renewable energy, but also improves the public perception of environmental consciousness towards mining.

1.2. Relevant Works

Relevant works on this domain are the works that discuss about employing solar technologies in mine sites and the energy storage technology that they opt for. Deployment of solar energy in mining is relatively a new topic, contrary to residential and commercial sectors. The first MW-scale solar PV system in a mine site was installed in 2012 at Cronimet's South African chromium ore operation generating up to 1.8 GWh of energy per year [20]. A historical breakthrough of solar penetration in mining took place in 2013 after the installation of a 10-MW solar thermal plant in a Copper mine in the Atacama Desert. Owned by Minera El Tesoro, the plant replaced more than 55% of the diesel fuel consumed in the heating process for electro-extraction of copper [21]. Musselwhite mine in Canada, Chevron molybdenum mine in the USA, and few other mines in Chile are utilizing solar energy in mine sites. As a matter of fact, many of the world's remote mine activities are located between 35° latitude north and south where the sun is intense and reliable [22]. An ice storage technology run on solar PV can aid in reducing the cooling plant maximum capacity in a Canadian mine [23]. Baig et al. [24] recommends four mine sites in the Northern Territory of Australia for Concentrating Solar Panel installation at the regional cluster level. Kim Trapani demonstrated the potential of floating solar panels in a remote McFaulds lake in Ontario to generate electricity of 400 MW that could provide electricity to 16 mines in this area [25]. A comprehensive literature review suggests that the solar technology is penetrating slowly but surely in the mining industry. However, most of the current and proposed applications include heating and electricity generation while only two publications are discovered for cooling [23,26].

Solar cooling has various technological options. Most widely investigated are solar electric and solar thermal. Before 2000, only solar thermal option was considered for chilling applications due to the high price of PV as compared to thermal collectors. However, the price in solar PV dropped by half from 2000 to 2010 and another halving took place from 2010 to 2015 [27]. The literature suggests that the Vapor Compression Refrigeration System (VCRS) based on solar electric has surpassed solar thermal schemes in 2013 [28–30]. Today, PV-driven solar cooling costs about half of the best thermally driven systems [27]. Different works of the literature are reported in solar electric cooling for diverse domestic applications [31–33]. However, applications in mining remain largely undiscovered.

Solar electric cooling couples VCRS with solar PV. Solar PV installed for industrial applications like mining, requires large scale energy storage systems to resolve the intermittency problem. A battery storage system, which stores energy in a chemical medium, is the most widely used solar energy storage technology [34]. However, in recent years, a new realm in solar refrigeration is added after the battery bank is completely replaced or partially substituted with Ice Thermal Energy Storage (ITES) system. In this scheme, energy is stored in ice which later is adapted for chilling purposes. The ITES from solar PV has a great advantage as it can be used in reducing peak refrigeration demand resulting in peak shaving and capital cost savings. Xu et al. [35] performed an experimental research on solar PVs operated as energy generators for ice thermal storage chillers for air-conditioning applications and concluded that a battery bank could completely be replaced by the ITES system. Axaopoulos and Theodoridis [33] successfully presented an autonomous battery-less solar-powered ice maker. Salilih et al. [36] performed an analysis and simulation of solar PV-driven VCRS in a real weather condition without battery storage. National Renewable Energy Laboratory (NREL) projects the energy storage cost in using Li-ion battery at a utility-scale solar PV is about 80% of the total cost of a PV

installation [37]. The average total annualized cost of a thermal storage system is about 12% of a Li-ion battery, while the efficiency is about half [38]. It would be interesting to compare these two energy storage technologies in an industry-scale refrigeration application.

This paper examines the techno-economic aspects of installing solar PV for operating an ice-generating machine to cool an underground mine. A thorough literature review suggests only two publications to study the use of solar energy in mine cooling applications [23,26]. Both of the analyses are performed for a specific mine site and are unsuitable to apply in decision making for the other mine locations. They also compare thermal storage strategies with a battery system but do not consider the battery replacement cost after standard charging and discharging cycles. This paper presents a detailed numerical code developed in Excel to design a solar PV system and to compare two different energy storage technologies for the proposed application: battery storage and ITES. A system-level analysis is performed for a PV-run refrigeration system capable of generating 200 tonne of ice per day. Carbon emission reduction is quantified in substituting a diesel-operated conventional refrigeration system with a solar-operated arrangement. The financial impact of substituting battery with ITES is performed in terms of cash flow analysis, capital cost, cumulative savings, and payback period considering the time value of money. To make an analysis independent of refrigeration requirement and mine locations, results are presented in terms of sun peak hours enabling easy decision making for investors. Finally, a sensitivity analysis is proposed to investigate the variation of solar intensity on energy and economic indexes.

2. Methodology

Solar PV is an integral component of the proposed ice refrigeration system, as shown in Figure 1. Electricity from solar PV operates the refrigeration plant to generate 200 tonne of ice per day. This ice can be fed into the vertical shafts of underground mines which later can be used for refrigeration purposes. A conveyer belt is used to carry ice from the refrigeration plant to the vertical shaft.
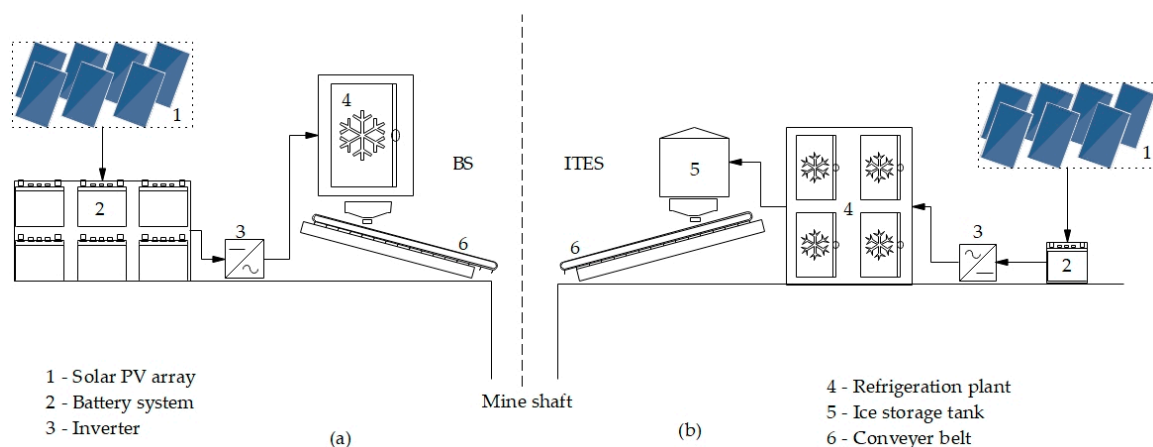

1 - Solar PV array
2 - Battery system
3 - Inverter

4 - Refrigeration plant
5 - Ice storage tank
6 - Conveyer belt

(a)　　Mine shaft　　(b)

Figure 1. (**a**). Flow schematics of Battery Storage System (BS) and (**b**). Flow schematic of Ice Thermal Energy Storage System (ITES).

The refrigeration plant is assembled in two unique configurations. These two different arrangements with corresponding component denomination are presented as options 1 and 2 in Figure 1. In both configurations, solar PV is used to generate electricity that ultimately powers the refrigeration plant. The configurations only differ in terms of their internal design aspects; however, they should still share many commonalities (i.e., number of conveyor belts, size of PV required, and so on.) In option 1, DC from solar PV is stored in a lithium-ion battery bank that is connected to the inverter. This inverter provides AC power needed to operate the refrigeration plant. Then, the refrigeration plant generates ice to be fed to the vertical intake shaft with the help of conveyors and belt system. Option 2 is different than option 1 in terms of the battery bank and the ice

storage tank. The battery bank in option 2 is smaller as compared to option 1 and only acts as a buffer stock between solar panel and compressor of the refrigerator. Here, the use of the battery is just to supply the constant voltage with minimum noise, and the initial surge current requirement rather than energy storage. It is significant to note that option 2 can only operate during sun hours and the system is designed to generate a fixed amount of cooling per day (200 tonne of ice). Hence, the capacity factor of the refrigeration plant for this system is lower than the option 1 it requires a greater number of refrigerators. In option 2, ice generated from solar configuration is stored in the storage tank which later is used for refrigeration purposes during evening or night hours when there is no sun in the sky. For convenience, option 1 is referred to as Battery Storage System (BS) and option 2 is referred to as Ice Thermal Energy Storage System (ITES) hereafter.

2.1. State-of-the-Art Comparison

State-of-art technology is used in designing the solar-refrigeration system. Components with improved durability and lowered costs, and which are available in the market are employed. Today, independently confirmed efficiencies of solar cells and modules are easily higher than 20% [39]; however, the industrially manufactured solar modules have an efficiency in the range of about 20%. The PV module used in this analysis is a poly-crystalline module with an efficiency of 19.2% [40]. Several companies in Europe and America manufacture ice-generation refrigerators for different applications ranging from concrete cooling to mine cooling to fish processing to beverage cooling. These machines can generate ice from the water with a temperature of up to 35 °C and an ambient temperature as high as 40 °C [41]. Similarly, several companies manufacture industrial-scale ice storage systems that could store any type of ice for several days. The typical size of these devices ranges from 20 to 250 tonne per container. They have a fully automatic ice discharge system with a conveyer belt and are suitable for standard or tropical climate. The refrigeration plant and the ice storage system considered for this analysis are manufactured by KTI-Plersch Kältetechnik, Germany. These refrigerator plants rely on ammonia as a refrigerant, and have a designed evaporator temperature of −13 °C and can generate pure ice from the intake water [42]. Lead-acid batteries were the best options for solar PV systems a few years ago. However, with recent developments in technology, lithium-ion batteries outperformed lead-acid batteries [43,44]. In addition to a higher life, they have low losses and extended cycle life with lower storage depletion rates as compared to lead-acid batteries [45]. Hence, in this analysis, the lithium-ion batteries with a battery management system is used.

2.2. Mathematical Modeling

2.2.1. Solar PV Design

Mathematical modeling of the system starts with the rated power of the refrigerator. This rated AC power of the machine is obtained from the manufacturer datasheet and is denoted as P_{rated}. The power needed is provided by the solar PV and battery system which is connected to the refrigerator through inverter of efficiency η_{inv}. With this efficiency, the maximum power needed in DC from the solar system is calculated using Equation (1). Inverter efficiencies of up to 99% can be found thanks to the research and development in power electronics. Inverter used in this analysis has a DC-to-AC ratio of 1.0 and an efficiency of 97% [46].

$$\text{Maximum power required in } DC \ (P_{max,\ DC}) = \frac{P_{rated}}{\eta_{inv} \times DC - AC \ ratio} \qquad (1)$$

This power is consumed by the refrigeration machine throughout a day to generate 200 tonne of ice. Consequently, the total energy required in kWh by the system per day is calculated by using Equation (2).

$$\text{Total energy demand per day in } DC \ (E_{total}) = P_{max,DC} \times 24 \qquad (2)$$

This is the total amount of energy to be generated using solar PV each day. The solar system is designed to be a stand-alone solar power system. Solar PV module chosen for this application is a 400 W poly-crystalline module manufactured by Canadian solar with a rated efficiency of 19.2% [40]. Electrical data including optimum operating voltage and optimum operating current are obtained from the datasheet available from the manufacturer. To calculate the design operating voltage, Equation (3), a voltage efficiency of 90% is used. This analysis is performed to ensure acceptable module output current which is less than optimum operating current.

$$\text{PV operating voltage} \left(V_{operating} \right) = V_{opt.\ power\ voltage} \times \eta_{voltage} \tag{3}$$

The guaranteed power output from a single PV module at STC is obtained from relation (4) with a safety factor of 1.10. This number is also verified from the I–V curve available from the manufacturer's datasheet.

$$\text{Gurrented power} \left(P_{gurrented} \right) = \frac{V_{operating} \times I_{operating}}{S.F.} \tag{4}$$

Output power from a solar PV also depends on ambient operating temperature. So, thermal efficiency is accounted for obtaining an output power form PV by using Equation (5). An equation to determine the thermal efficiency of the module is given by Equation (6). Proposed by Evans [47], β_{ref} in the equation represents the temperature coefficient of the module, while T_c and T_{ref} are the solar cell temperature and reference temperature respectively. Since, the system is not designed for specific mine location, no ambient temperature data is available to calculate exact thermal efficiency of the system. Thermal efficiency considered for this design analysis is 90%.

$$P_{operating} = P_{gurrented} \times \eta_{thermal} \tag{5}$$

$$\eta_{thermal} = \left[1 - \beta_{ref} \left(T_c - T_{ref} \right) \right] \tag{6}$$

Total energy output from each module per day is calculated using peak sun hours for the desired location using Equation (7) with a safety factor of 1.10. Peak sun hours (SH_{Peak}) is the number of hours during which the intensity of sunlight is 1000 W/m^2 for that specific place per day. The code is developed in such a way that; with the input of sun peak hours for any mine location, a system feasibility result can be concluded.

$$E_{per\ module\ per\ day} = \frac{P_{operating} \times SH_{peak}}{S.F.} \tag{7}$$

Using this number, the total number of modules required to meet the energy demand is calculated using Equation (8)

$$N_{total} = \left(\frac{E_{total}}{E_{per\ module\ per\ day}} \right) \tag{8}$$

Equation (9) gives the number of modules required per string. These are the numbers of solar panels that should be connected in series to provide an adequate voltage to the battery supply. This is also equal to the inverter input DC voltage supply.

$$N_{series} = \frac{V_{inverter,\ DC}}{V_{operating}} \tag{9}$$

The total number of strings in parallel is calculated by using the following relation (10). In computing the number of series and parallel panels, every panel number is adjusted to the next higher integer.

$$N_{parallel} = \frac{N_{total}}{N_{series}} \tag{10}$$

Finally, nominal rated array output is calculated using Equation (11). This is the rated module output in watts as per the manufacturer.

$$\text{Nominal rated array output} = N_{total} \times PV_{rated\ power} \tag{11}$$

The total area of the solar field required is calculated by multiplying the individual area of the solar panel with total numbers of solar panels as following. A solar panel used is of size $2108 \times 1048 \times 40$ mm in dimensions.

$$\text{Total area of solar field} = N_{total} \times \text{area of a module} \tag{12}$$

2.2.2. Battery System Design

The solar system can generate the energy required to operate the machine by converting energy from the sunlight into a flow of electrons using the photovoltaic effect. However, this energy is generated only when there is solar irradiation. This section describes the design of the battery bank, which is the essential component for BS. The total energy required for the refrigeration machine from Equation (2) is used as a design criterion for the battery bank. This amount of energy is to be supplied by the battery system in a single day to operate the system efficiently. This battery storage system is designed independently from the photovoltaic array. To size the battery bank, the total electrical load is converted from watt-hours to amp-hours. Battery capacity in amp-hours is calculated by using Equation (13).

$$\text{Total amp-hour demand per day} = \frac{E_{total\ required} \times 1000}{Battery_{bus\ voltage}} \tag{13}$$

This battery bus voltage provides the nominal operating DC for the system. The battery bus voltage for this application is picked as 600 V, which also corresponds to the DC input voltage for the inverter. The maximum fraction of capacity that can be withdrawn from the battery, also known as the allowable depth of discharge, is considered in designing the battery system. For this application, 0.8 depth-of-discharge is considered. This gives the actual required battery capacity, as shown in Equation (14).

$$\text{Actual battery capclity} = \frac{Total\ amp\text{-}hour\ demand\ per\ day}{depth\text{-}of\text{-}discharge} \tag{14}$$

Once the total required capacity of the battery bank is estimated, the battery to be used in the system is selected. The Tesla Powerball battery specification data sheet is used for the selection of the battery. Accordingly, the battery selected in this case has a usable energy storage capacity of 13.5 kWh. The total number of batteries in series and parallel is given by the Equations (15) and (16).

$$N_{parallel} = \frac{\text{Actual battery capacity}}{\text{amp-hour capacity of selected battery}} \tag{15}$$

$$N_{series} = \frac{\text{Battery bus voltage}}{\text{voltage of selected battery}} \tag{16}$$

Batteries in series are arranged in such a way that the DC voltage provided by the battery system corresponds to the inverter DC input voltage. Additionally, the number of batteries in parallel is fixed to provide the battery required capacity. The overall idea is to make sure that the required amp-hour is supplied with the required voltage supply. Equations (17) and (18) provide the total number of batteries required and total battery capacity, respectively.

$$N_{total} = N_{series} \times N_{parallel} \tag{17}$$

$$\text{Total battery capacity} = N_{total} \times \text{Usable energy of single battery} \tag{18}$$

2.2.3. Calculations of Savings

In this section, power savings, energy savings, diesel savings, reductions in carbon emissions, and carbon tax savings are quantified. Here, rated AC power of the refrigerator is used as a reference to perform an analysis. Energy savings per year in kWh is given by Equation (19),

$$E_{savings} = Power_{savings} \times 24 \times 365 \tag{19}$$

The equivalent amount of diesel savings is calculated by converting energy savings to joules and dividing by the calorific value of diesel. The calorific value of diesel used in this analysis is 35.9 MJ/liter [48]. The efficiency of a diesel generator is accounted for in calculating the total amount of energy used. In this study, the efficiency of the diesel generator is used as 33% and the amount of diesel savings is given by Equation (20).

$$Diesel_{savings} = \frac{E_{savings}}{calorific\ value \times \eta_{generator}} \tag{20}$$

The quantification of diesel emission is made based on the amount of diesel saved over a year. This quantity is given by relation (21). For this calculation, an emission rate of 2.63 kg of CO_2 per liter of diesel is used while a carbon tax rate of USD 35 per tonne of CO_2 is used in the analysis [16].

$$CO_2\ savings = quantity\ of\ diesel\ savings \times emission\ per\ liter \tag{21}$$

Finally, total cost savings is the summation of energy cost savings from diesel generators and carbon savings. This is calculated by using formula (22).

$$Cost\ savings = \left(Energy_{savings} \times Diesel\ cost\right) + \left(CO_2\ emissions \times carbon\ tax\right) \tag{22}$$

2.2.4. Economic and Financial Calculations

Net Present Value (NPV) of the project is calculated based on Equation (23), where i is the discount rate and F_n is the net cash flow in year n. Net cash flow is the difference between net savings and net expenditure over the year. Net savings include the savings from energy and carbon emissions savings, while the net expenditure includes the capital cost, principal and interest payment, and Operation and Maintenance cost.

$$NPV = \sum_{n=0}^{N} \frac{F_n}{(1+i)^n} \tag{23}$$

Annual loan payment for the project is calculated using the following Formula (24), where i and n are interest rate and the loan payback period in years, respectively.

$$Annual\ loan\ payment\ amount = Total\ loan\ amount \times \left[\frac{i \times (1+i)^n}{(1+i)^n - 1}\right] \tag{24}$$

Levelized cost of energy (LCOE) is that cost that, if assigned to every unit energy produced by the system over the analysis period, will equal the total life-cycle cost of the project discounted back to the base year. LCOE is calculated using an Equation (25). The numerator in Equation (25) represents all costs of the project over its life while the denominator is the total energy generated from the project over its life, both converted to a present value. Here, C_n is the total cost and Q_n is the energy produced in year n.

$$LCOE = \frac{\sum_{n=0}^{N} \frac{C_n}{(1+i)^n}}{\sum_{n=1}^{N} \frac{Q_n}{(1+i)^n}} \tag{25}$$

Table 1 summarizes the different economic parameters used in the analysis. The solar installation and system commissioning time is assumed to take a year. For both systems, half of the total capital cost comes from the company's equity whereas another half from a loan. The borrowed loan is paid back in 10 equal installments in 10 years from the time after the system is commissioned. This loan repayment schedule is also known as 'even total payment' method. The installation cost of PV and battery systems are obtained from the National Renewable Energy Laboratory (NREL) report as of 2018 pricing structure [37]. Additionally, the cost of the panel, inverter, and battery is verified with other manufacturing companies [46,49–51]. The cost of a refrigeration plant and its accessories are obtained from a plant manufacturing company. Fixed cost, variable cost, direct cost, and indirect cost associated with the project execution are also accounted for in the analysis. The proposed system assumes that the solar system and battery system are co-located. The cost of the solar system is expressed in USD/kW while the cost of the storage system in USD/kWh and the cost of refrigeration plant in USD/tonne of ice generation.

Table 1. Economic evaluation parameters of proposed systems.

Time Parameters		Solar Cost Share (USD per W)		Battery Cost Share (USD per kWh)	
Analysis year	2020	Solar Panel	0.47	Battery	209
Year construction starts	2020	Inverter	0.08	Structural	13
Construction period (year)	1	Structural and electrical	0.25	Electrical	36
Project life (years)	20	Installations and labor	0.13	Installations and labor	23
Inflation/discount rate (%)	2	Shipping and handling	0.16	Shipping and handling	12
Financing Parameters		PII	0.09	PII	8
Equity (%)	50	Sales tax	0.05	Sales tax	22
Loan (%)	50	Developer overhead	0.36	Developer overhead	10
Financing rate (%)	8	Contingency	0.04	Contingency	10
Loan term years	10	Developer net profit	0.11	Developer net profit	18
Salvage factor (%)	5	Total	1.74	Total	361

Note: PII = Construction permitting, interconnection, testing, and commissioning.

3. Results and Discussions

3.1. Solar PV

The total power drawn by the compressor and its accessories is 443 kW, which provides a cooling capacity of 1.2 MW with a COP of 2.8. To run this device merely with solar system, nominal array output of 2.5 MW is needed for a place with 6-h of sun peak. Since most of the remote mines are located in high solar intensity zones, this solar irradiation intensity is considered as a standard number and is used in analysis hereafter. Additionally, 3.4 acres of land is needed to install the proposed solar photovoltaic system. Figure 2 illustrates the design change in the solar PV system, and the corresponding change in the Levelized Cost of Energy (LCOE) and the area of the solar field required for different sun peak hours. As expected, there is a strong correlation between solar intensity, LCOE, and the area of the solar field required associated with sun peak hours. An increase in sun peak hours leads to an obvious decrease in installation capacity, LCOE, and area of installation field required.
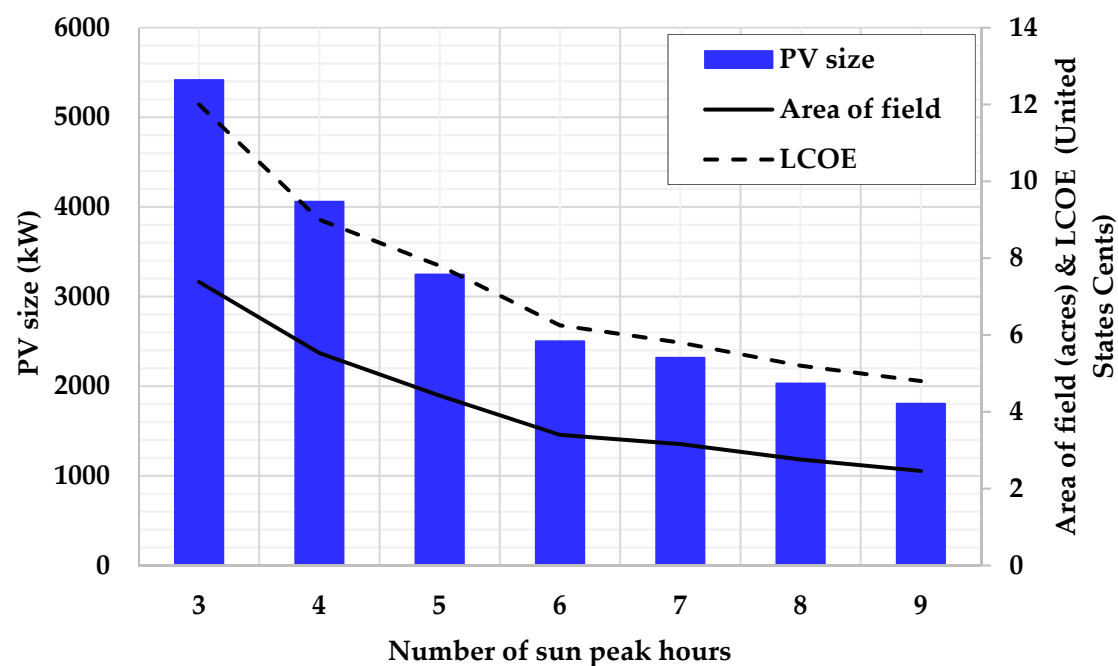
Figure 2. PV size, Levelized Cost of Energy (LCOE), and area variation with solar intensity.

3.2. Battery

To operate a refrigeration plant for a day, 11.5 MWh of energy is required. This energy is to be stored in the battery bank. The battery bank is designed with an allowable depth of discharge of 0.8 and provides 600 V of battery bus voltage to the inverter. With these design criteria, the total battery capacity of 23.9 KA-h and 14.3 MWh is required to operate the system. However, in designing the battery system, since the refrigeration plant is in operation throughout the day, the only energy required to operate the system during no-sun hours is to be stored in the battery bank. That means, the refrigerator is in operation during the sunshine hours for which the energy is not stored. With this approach, the total battery capacity required for the system is 10.6 MWh and 17.9 KA-h.

3.3. Savings

Table 2 summarizes the key technical findings, along with the annual savings after the project comes to execution. On replacing the conventional refrigeration system with a solar-powered refrigeration system, total energy savings of 10.6 MWh per day is achieved. It is worth mentioning that this savings is just for a single refrigeration unit. If multiple units are to be used depending on the refrigeration demand, this number will get multiplied accordingly. Similarly, energy savings per year per unit is 3.9 GWh. In addition, considering capital cost and operation and maintenance cost, the Levelized Cost of Energy (LCOE) from the solar system is calculated as USD 0.06/kWh. This energy is achieved at the cost of 1180 Kilo liters of diesel with a diesel generator running at an efficiency of 33%. The calorific value of diesel considered is 35.9 MJ/liter [48]. With global average diesel price [52], and including transportation and storage costs, total savings from fuel is USD 0.95 million per annum. Unit cost of diesel per liter is USD 0.81 and the cost of energy from diesel generator is calculated as USD 246 per MWh. Moreover, electricity generated from diesel plants is ineffective and comes at the cost of significant environmental risks. These risks may be associated with diesel particulate matter, vapor, and greenhouse gases. Although the effect of particulates and vapor is not accounted for, the GHG emission effect is evaluated. A total of 2.63 kg of CO_2 is released per liter of diesel combustion [16] and a total emission of 3103 tonne is saved in penetrating solar system to run a refrigerator. With a carbon tax rate of USD 35 per tonne of CO_2, total carbon savings is computed to USD 108k per annum.

Table 2. Key technical findings.

S.N.	Variable	Value	Unit
1	Solar PV capacity	2.5	MW
2	Energy storage capacity	10.6	MWh/day
3	Levelized Cost of Energy from PV	0.06	USD/kWh
4	Energy savings from Diesel	3.9	GWh/year
5	Diesel savings	1180	Kilo liter/year
6	Total cost of diesel per liter	0.81	USD
7	Diesel energy cost per MWh	246	USD
8	Carbon emission savings	3103	Tonne/year
9	Operating expenses savings	1.1	million (USD)/year

3.4. Capital Cost

With the cost breakdown from Table 1, the total capital cost of the project is calculated. Figure 3 depicts the waterfall chart showing the capital cost requirement for two different scenarios. The total initial investment for solar panel and its accessories is found to be USD 4.3 million including AC/DC inverter. With the battery management cost included, the capital cost of the battery system is calculated as USD 3.8 million. Considering the decrease in electrochemical performance during charging and discharging cycles of the lithium-ion battery, battery replacement is required every 10 years or after 3600 cycles [53]. Therefore, for the battery-based system, an additional cost is needed at the end of each 10-year operational period. This is shown as 'battery replacement' cost in Figure 3b. The price of lithium-ion batteries after 10 years is projected based on the available published resources [54–56], and accounting the time value of money. The capital cost of a single refrigeration plant is USD 910k including installation and commission charge. The storage cost of ice is USD 32 per kWh and the total cost of the required storage system is USD 350k [38]. For ITES, a small amount of battery is required to supply sufficient voltage and current for the refrigerator. This number at least should be equal to the number of batteries in series given by Equation (15). However, to be on the safe side, the battery system is designed to supply continuous energy demand for half an hour. Corresponding total cost of such a designed battery system is USD 100k.
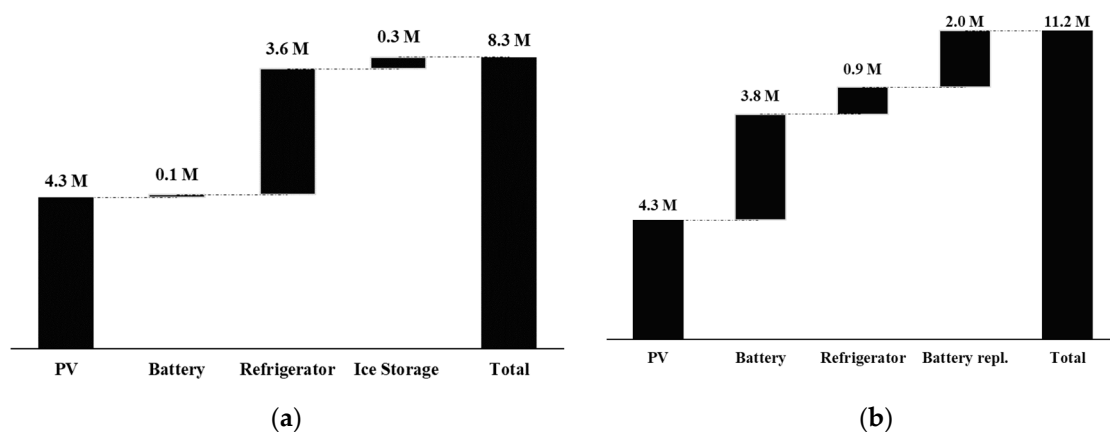
Figure 3. (**a**) Capital cost breakdown for ITES and (**b**) Capital cost breakdown for BS.

Clearly, the investment cost of BS is higher than that of ITES. Although both systems shown here share the same solar PV cost, the difference can be attributed to the battery cost. Another important point that should be noted is the cost of a refrigerator in an ITES. The refrigeration cost for this option is four times the BS. As mentioned earlier, both systems are designed to generate an equal amount of ice each day, and ITES does not have a battery bank to operate during non-sun hours. Hence, to ensure the required amount of ice generation, multiple refrigerators should be used. This analysis assumes

the number of sun-peak sours to be six, hence four such refrigerators are needed which increases the capital cost of refrigerators in ITES.

3.5. Cash Flow Analysis

The financial model of the analysis considers that half of the total investment cost in both cases is from the company's equity while the remaining half is loaned from a financial institution. As mentioned in Table 1, inflation and interest rates used in the analysis are 2% and 8%, respectively [57]. With this hypothesis, as can be inferred from Table 3, the total financed amount is equal to USD 4.1 million in ITES and USD 5.6 million in BS. In both cases, loan financing is done at the beginning of the project and is paid back in 10 equal installments over the first 10 years after the project comes in operation. Although the total capital cost of the project is higher in BS, this amount also includes the battery replacement cost that will take place after 10 years of operation. It is worth mentioning that the useful life of the mine considered is 20 years and the economics will change for a shorter or longer mine lifecycle period. Since half of the total project investment comes from a loan at the beginning of the project, battery replacement cost is the part of company's equity. Due to this reason, as shown in Table 3, initial equity in ITES is considered as USD 4.1 million, which accounts for USD 500k more than of BS' equity share. Although the equity amount of ITES at the beginning is more than that of BS, due to the larger loan amount, annual loan payment of the project is higher in BS than ITES by USD 218k.

Table 3. Key economic findings (Currency: USD).

| Option | Total Capital Cost | Loan | Equity | | Annual Loan Payment | Total Savings | Payback Period |
		Year '0'	Year '0'	Year '10'			
ITES	8.3 million	4.1 million	4.1 million	-	612k	7.8 million	10 years
BS	11.2 million	5.6 million	3.6 million	2.0 million	830k	4.8 million	13 years

Figures 4 and 5 represent the net cash flow diagram for two different setups. The red color in the figures indicates the net cash outflow, while the green color represents total cumulative savings at the end of each fiscal year. Cash outflow includes capital cost, loan payment (principal and interest), and operation and maintenance cost while cumulative savings is the operating income from annual savings. Net Present Values are used in calculating cumulative savings for a sound economic comparison. As bank loan is paid in the first 10 years, cash outflow after the 10th year represents only operation and maintenance costs. Year 'zero' is the construction year and no savings are made until the project comes in operation, which is at the beginning of the year 'one'. This means, cash flow in year 'zero' refers only to the initial investment made from the company's equity. It should be recalled that both proposed systems generate equal cooling effect irrespective of the energy storage technology chosen. This results in an equal amount of operating income or savings over a year. Equal annual savings with unequal loan payment amount results in different cumulative savings over the period.

As depicted in Figures 4 and 5, investing in ITES returns more savings. With project implementation, at the end of the project life, total savings for BS and ITES are estimated at USD 4.8 million and 7.8 million, respectively.

Hence, from the company's viewpoint, with an initial equity investment of USD 4.1 million, ITES pays USD 7.8 million in total at the end of the project. On the other hand, BS returns only USD 4.8 million for an initial investment of 5.6 million. This indicates that both options are in profit at the end of the project. But, while comparing these two systems, cumulative savings for the ITES is greater than the BS by USD 3.0 million.

Cash flow diagram also depicts the payback period for both projects. As initial equity of the ITES is higher than the BS by USD 500k, the cumulative saving of ITES is more negative than BS at the beginning of the project. But once the project comes in operation, things go in the opposite direction due to more amount of loan payment in BS. One more factor to deaccelerate the payback period of the BS is the additional capital requirement in replacing the Li-ion battery at the end of the

10th year. This decreases the cumulative savings by USD 2 million and hence increases the payback period. For ITES, a period of 10 years is enough to pay back the investment. However, this time increases to 13 years for the BS due to larger capital size and higher annual loan of the associated system. Hence, the ITES storage system is a better option out of two considered alternatives in terms of cumulative savings and payback period.
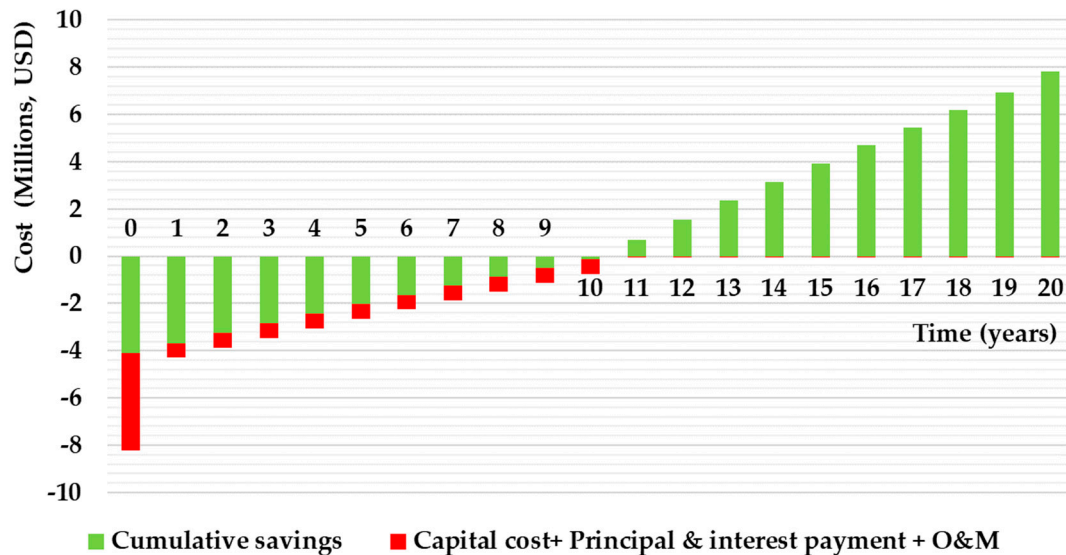

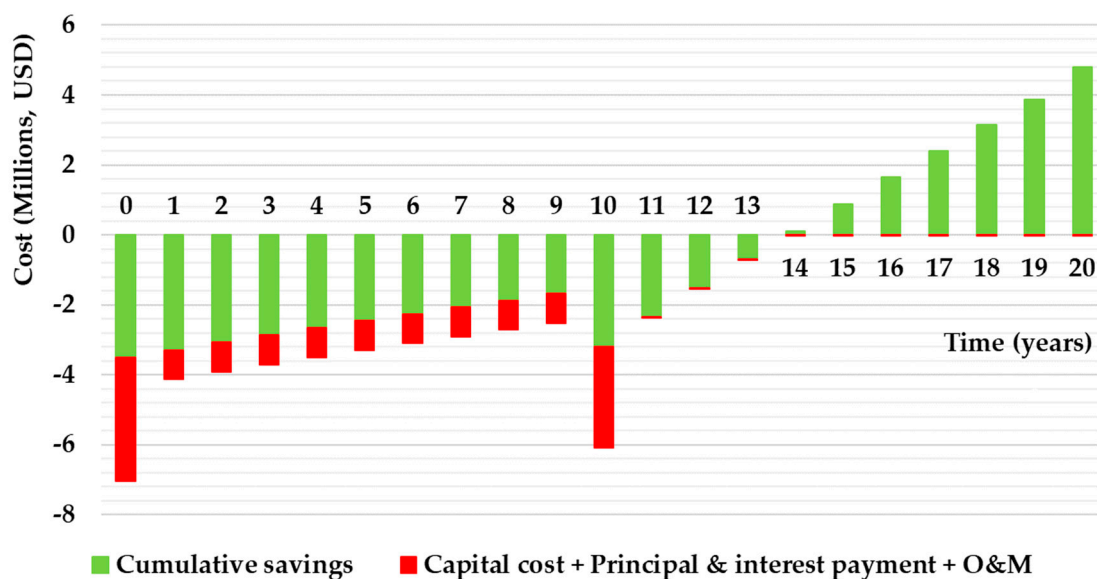
Figure 4. Cash flow diagram for ITES.

Figure 5. Cash flow diagram of BS.

4. Conclusions

This techno-economic analysis explored the potential of using solar photovoltaics in cooling remote underground mines. The proposed solar system provides electric energy to operate a refrigeration unit capable of generating 200 tonne of ice per day. The study finds that to generate a cooling effect of 8.3 MWh per day, 2.5 MW of solar photovoltaics should be installed in a place with an average sun-peak hour of 6. The Levelized Cost of Energy from solar PV for a project with a life of 20 years is found as 0.06 USD/kWh. The penetration of the solar system could save the carbon footprint by 3100 tonne per year in addition to 1180k liters of diesel. Two scenarios are developed in storing the

electric energy from the solar system: Ice Thermal Energy Storage System (ITES) and Battery Storage system (BS). Economic analysis suggests that capital cost of USD 11.2 million is required to establish the BS which is about USD 2.9 million greater than ITES. While both systems return enough to pay back the investment during their lifetime, a higher initial investment cost leads to a relatively slower payback period for BS. While ITES pays back in 10 years, BS takes 13 years to pay back the amount invested. In addition, ITES and BS generate cumulative savings of USD 7.8 million and USD 4.8 million respectively at the end of the project lifetime.

In conclusion, this paper recommends the use of solar PV for mine cooling applications in places with average sun peak hours of 6 or greater. Besides, Ice Thermal Energy Storage System is recommended over Battery System due to lower capital investment cost, higher savings, and a smaller payback period.

Author Contributions: S.P.: Conceptualization, investigation, methodology, software, validation, writing—original draft, writing—review & editing. A.F.K.: conceptualization, validation, writing—review & editing. H.K.: conceptualization, validation, writing—review & editing. S.A.G.-M.: conceptualization, validation, resources, supervision, writing—review & editing. All authors have read and agreed to the published version of the manuscript.

Funding: This research received no external funding.

Conflicts of Interest: The authors declare no conflict of interest.

References

1. Energy Information Administration. *International Energy Outlook 2019 with Projections to 2050*; Energy Information Administration: Washington, DC, USA, 2019.
2. International Energy Agency. *World Energy Statistics 2018*; International Energy Agency: Paris, France, 2018; p. 860.
3. Bluhm, S. Improving Mine Ventilation Electricity Consumption. *Mining Review Africa.* 26 September 2008. Available online: https://www.miningreview.com/top-stories/improving-mine-ventilation-electricity-consumption/ (accessed on 26 August 2020).
4. Stephenson, D. Distribution of water in deep gold mines in South Africa. *Mine Water Environ.* **1983**, *2*, 21–30. [CrossRef]
5. Biffi, M.; Stanton, D.; Rose, H.; Pienaar, D. Ventilation strategies to meet future needs of the South African platinum industry. *J. S. Afr. Inst. Min. Metall.* **2007**, *107*, 59–66.
6. Norgate, T.; Haque, N. Energy and greenhouse gas impacts of mining and mineral processing operations. *J. Clean. Prod.* **2010**, *18*, 266–274. [CrossRef]
7. Zietsman, L.N.; Marais, J.H.; Joubert, H.P.R. Identification model for cost-effective electricity savings on a deep-level mine surface refrigeration system. In Proceedings of the 2018 International Conference on the Industrial and Commercial Use of Energy (ICUE), Cape Town, South Africa, 13–15 August 2018; pp. 1–6.
8. Du Plessis, G.E.; Arndt, D.C.; Mathews, E.H. The development and integrated simulation of a variable water flow energy saving strategy for deep-mine cooling systems. *Sustain. Energy Technol. Assess.* **2015**, *10*, 71–78. [CrossRef]
9. Nel, A.; Van Rensburg, J.F.; Cilliers, C. Improving existing DSM initiatives on mine refrigeration systems for sustainable performance. In Proceedings of the 2017 International Conference on the Industrial and Commercial Use of Energy (ICUE), Cape Town, South Africa, 15–16 August 2017; pp. 1–7.
10. Schutte, A.; Kleingeld, M.; Van Der Zee, L. An integrated energy efficiency strategy for deep mine ventilation and refrigeration. In Proceedings of the 2014 International Conference on the Eleventh industrial and Commercial Use of Energy, Cape Town, South Africa, 19–20 August 2014; pp. 1–9.
11. Mining Technology. *Ice Cooling Takes the Heat Off at Harmony's Phakisa Gold Mine*; Mining Technology: London, UK, 2015; pp. 1–3. Available online: https://www.mining-technology.com/features/featureice-cooling-takes-the-heat-off-at-harmonys-phakisa-gold-mine-4454482/ (accessed on 26 August 2020).
12. Mackay, L.; Bluhm, S.; van Rensburg, J. Refrigeration and cooling concepts for ultra-deep platinum mining. *S. Afr. Inst. Min. Metall.* **2010**, *4*, 285–292.

13. de Wet, J.; Mackay, L.; Bluhm, S.; Walter, K. Refrigeration and ventilation systems for ultra-deep platinum mining in the bushveld igneous complex. In Proceedings of the 10th International Mine Ventilation Congress, Sun City, South Africa, 2–8 August 2014; pp. 1–8.

14. Belle, B.; Biffi, M. Cooling pathways for deep Australian longwall coal mines of the future. *Int. J. Min. Sci. Technol.* **2018**, *28*, 865–875. [CrossRef]

15. Van Der Walt, J.; De Kock, E. Developments in the engineering of refrigeration installations for cooling mines. *Int. J. Refrig.* **1984**, *7*, 27–40. [CrossRef]

16. International Energy Agency. *CO2 Emissions from Fuel Combustion*; International Energy Agency: Paris, France, 2017.

17. McLellan, B.; Corder, G.D.; Giurco, D.P.; Ishihara, K. Renewable energy in the minerals industry: A review of global potential. *J. Clean. Prod.* **2012**, *32*, 32–44. [CrossRef]

18. Sullivan, G. *Diverging from Diesel: The True Cost of Diesel Power in the Canadian North*; Gwich'in Council International: Whitehorse, YT, Canada, 2017; Available online: https://www.rncan.gc.ca/sites/www.nrcan.gc.ca/files/energy/energy-resources/Diverging_from_Diesel_-_Technical_Report_FINAL.pdf (accessed on 16 July 2020).

19. Pretorius, J.G.; Mathews, M.J.; Maré, P.; Kleingeld, M.; Van Rensburg, J. Implementing a DIKW model on a deep mine cooling system. *Int. J. Min. Sci. Technol.* **2019**, *29*, 319–326. [CrossRef]

20. Judd, B.E. *Cronimet Mining-Power Solutions Completes World's First One-Megawatt Diesel-Pv Hybrid in South Africa*; Renewables and Mining Summit; Energy and Mines: Johannesburg, South Africa, 2014; Available online: https://energyandmines.com/wp-content/uploads/2014/05/Cronimet.pdf (accessed on 18 July 2020).

21. Awuah-Offei, K. *Energy Efficiency in the Minerals Industry*; Springer: Berlin, Germany, 2018.

22. Paraszczak, J.; Fytas, K. Renewable energy sources—A promising opportunity for remote mine sites? *Renew. Energy Power Qual.* **2012**, *1*, 251–256. [CrossRef]

23. Ghoreishi-Madiseh, S.A.; Kuyuk, A.F.; Kalantari, H.; Sasmito, A.P. Ice versus battery storage: A case for integration of renewable energy in refrigeration systems of remote sites. *Energy Procedia* **2019**, *159*, 60–65. [CrossRef]

24. Baig, M.H.; Surovtseva, D.; Halawa, E. The Potential of Concentrated Solar Power for Remote Mine Sites in the Northern Territory, Australia. *J. Sol. Energy* **2015**, *2015*, 1–10. [CrossRef]

25. Campbell, H. Solar power proposed for remote mines. *Sudbury Min. Solut. J.* **2011**, *8*, 18–19.

26. Othman, R. Thermal and Electrical Energy Storage Comparison Study for Mine Cooling. Engineering Thesis, Faculty of Engineering Architecture and Information Technology, The University of Queensland, Brisbane, Australia, 2018.

27. Lazzarin, R.; Noro, M. Past, present, future of solar cooling: Technical and economical considerations. *Sol. Energy* **2018**, *172*, 2–13. [CrossRef]

28. Kim, D.-S.; Ferreira, C.I. Solar refrigeration options—A state of the art review. *Int. J. Refrig.* **2008**, *31*, 3–15. [CrossRef]

29. Otanicar, T.; Taylor, R.A.; Phelan, P.E. Prospects for solar cooling—An economic and environmental assessment. *Sol. Energy* **2012**, *86*, 1287–1299. [CrossRef]

30. Ferreira, C.I.; Kim, D.-S. Techno-economic review of solar cooling technologies based on location-specific data. *Int. J. Refrig.* **2014**, *39*, 23–37. [CrossRef]

31. Rajoria, C.S.; Singh, D.; Gupta, P.K. Performance evaluation of solar photovoltaic panel driven refrigeration system. *IOP Conf. Ser. Mater. Sci. Eng.* **2018**, *330*, 012133. [CrossRef]

32. Modi, A.; Chaudhuri, A.; Vijay, B.; Mathur, J. Performance analysis of a solar photovoltaic operated domestic refrigerator. *Appl. Energy* **2009**, *86*, 2583–2591. [CrossRef]

33. Axaopoulos, P.J.; Theodoridis, M.P. Design and experimental performance of a PV Ice-maker without battery. *Sol. Energy* **2009**, *83*, 1360–1369. [CrossRef]

34. Department of Energy. *USA Battery Storage Market Trends*; Department of Energy: Washington, DC, USA, 2018.

35. Xu, Y.; Li, M.; Luo, X.; Ma, X.; Wang, Y.; Li, G.; Hassanien, R.H.E. Experimental investigation of solar photovoltaic operated ice thermal storage air-conditioning system. *Int. J. Refrig.* **2018**, *86*, 258–272. [CrossRef]

36. Salilih, E.M.; Birhane, Y.T. Modelling and performance analysis of directly coupled vapor compression solar refrigeration system. *Sol. Energy* **2019**, *190*, 228–238. [CrossRef]

37. Fu, R.; Remo, T.; Margolis, R. *2018 U.S. Utility-Scale Photovoltaics Plus-Energy Storage System Costs Benchmark*; No. NREL/TP-6A20-71714; National Renewable Energy Lab. (NREL): Golden, CO, USA, 2018.

38. Spataru, C.; Kok, Y.C.; Barrett, M. Physical Energy Storage Employed Worldwide. *Energy Procedia* **2014**, *62*, 452–461. [CrossRef]

39. Green, M.A.; Dunlop, E.D.; Levi, D.H.; Hohl-Ebinger, J.; Yoshita, M.; Ho-Baillie, A. Solar cell efficiency tables (version 54). *Prog. Photovolt. Res. Appl.* **2019**, *27*, 565–575. [CrossRef]

40. Canadian Solar. Super High Power Polyperc Module. 2020. Available online: https://www.canadiansolar.com/upload/55bb2d3819da47c6/0ac3c8f850d7224a.pdf (accessed on 12 November 2019).

41. THERMODIZAYN. Flake Ice Machine (Fresh Water). 2020. Available online: https://en.termodizayn.com/products/flake-ice-machine-fresh-water/ (accessed on 7 August 2020).

42. KTI. Ice Facilities. 2020. Available online: https://www.kti-plersch.com/de/produkte/kaelteanlagen-und-kuehlsysteme/eisanlagen/ (accessed on 26 July 2020).

43. Gurung, A.; Qiao, Q. Solar Charging Batteries: Advances, Challenges, and Opportunities. *Joule* **2018**, *2*, 1217–1230. [CrossRef]

44. Li, Q.; Liu, Y.; Guo, S.; Zhou, H. Solar energy storage in the rechargeable batteries. *Nano Today* **2017**, *16*, 46–60. [CrossRef]

45. Dhundhara, S.; Verma, Y.P.; Williams, A.A. Techno-economic analysis of the lithium-ion and lead-acid battery in microgrid systems. *Energy Convers. Manag.* **2018**, *177*, 122–142. [CrossRef]

46. ABB. ABB Central Inverters PVS800. 2011. Available online: https://new.abb.com/docs/librariesprovider22/technical-documentation/pvs800-central-inverters-flyer.pdf?sfvrsn=2 (accessed on 2 December 2019).

47. Evans, D. Simplified method for predicting photovoltaic array output. *Sol. Energy* **1981**, *27*, 555–560. [CrossRef]

48. Holmberg, K.; Erdemir, A. Influence of tribology on global energy consumption, costs and emissions. *Friction* **2017**, *5*, 263–284. [CrossRef]

49. Energysage. NHow Much Does Solar Storage Cost? *Understanding Solar Battery Prices.* 2019. Available online: https://www.energysage.com/solar/solar-energy-storage/what-do-solar-batteries-cost/#:~{}:targetText=Solarbatteriesrangefrom%245%2C000,kWh)to%24750%2FkWh (accessed on 11 April 2020).

50. Smartbattery. Lithium Ion Batteries. 2020. Available online: https://www.lithiumion-batteries.com/products/lithium-ion-solar-batteries/12v-300ah-lithium-ion-battery.php# (accessed on 11 April 2020).

51. Wholesale Solar. Shop Solar Panels. 2020. Available online: https://www.wholesalesolar.com/solar-panels (accessed on 11 April 2020).

52. USA EIA. Petroleum & Other Liquids. Independent Statistics and Analysis. 2019. Available online: https://www.eia.gov/petroleum/gasdiesel/ (accessed on 4 August 2020).

53. Smith, K.; Saxon, A.; Keyser, M.; Lundstrom, B.; Cao, Z.; Roc, A. Life prediction model for grid-connected Li-ion battery energy storage system. In Proceedings of the 2017 American Control Conference (ACC), Washington, DC, USA, 24–26 May 2017; pp. 4062–4068.

54. Cole, W.J.; Marcy, C.; Krishnan, V.K.; Margolis, R. Utility-scale lithium-ion storage cost projections for use in capacity expansion models. In Proceedings of the 2016 North American Power Symposium (NAPS), Denver, CO, USA, 20 September 2016; pp. 1–6.

55. Richa, K.; Babbitt, C.W.; Gaustad, G.; Wang, X. A future perspective on lithium-ion battery waste flows from electric vehicles. *Resour. Conserv. Recycl.* **2014**, *83*, 63–76. [CrossRef]

56. Claire, C. Lithium-ion Battery Costs and Market. 2017. Available online: https://data.bloomberglp.com/bnef/sites/14/2017/07/BNEF-Lithium-ion-battery-costs-and-market.pdf (accessed on 16 July 2020).

57. Krishan, O.; Suhag, S. Techno-economic analysis of a hybrid renewable energy system for an energy poor rural community. *J. Energy Storage* **2019**, *23*, 305–319. [CrossRef]